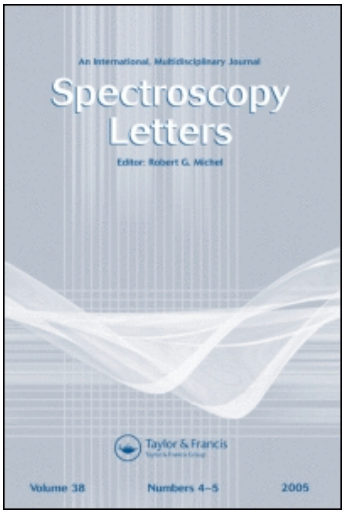

Spectroscopy Letters
Publication details, including instructions for authors and subscription information:
http://www.informaworld.com/smpp/title~content=t713597299

Tandem Mass Spectrometric Analysis of the Novel Gemini Surfactant Nanoparticle Families G12-s and G18:1-s

Joshua Buse[a]; Ildiko Badea[a]; Ronald E. Verrall[b]; Anas El-Aneed[a]
[a] Drug Design and Drug Discovery Research Group, College of Pharmacy and Nutrition, University of Saskatchewan, Saskatoon, SK, Canada [b] Department of Chemistry, University of Saskatchewan, Saskatoon, SK, Canada

Online publication date: 06 August 2010

To cite this Article Buse, Joshua , Badea, Ildiko , Verrall, Ronald E. and El-Aneed, Anas(2010) 'Tandem Mass Spectrometric Analysis of the Novel Gemini Surfactant Nanoparticle Families G12-s and G18:1-s', Spectroscopy Letters, 43: 6, 447 — 457
To link to this Article: DOI: 10.1080/00387010903261206
URL: http://dx.doi.org/10.1080/00387010903261206

Spectroscopy Letters, 43:447–457, 2010

ISSN: 0038-7010 print/1532-2289 online
DOI: 10.1080/00387010903261206

Taylor & Francis
Taylor & Francis Group

Tandem Mass Spectrometric Analysis of the Novel Gemini Surfactant Nanoparticle Families G12-s and G18:1-s

Joshua Buse[1], Ildiko Badea[1], Ronald E. Verrall[2], and Anas El-Aneed[1]

[1]Drug Design and Drug Discovery Research Group, College of Pharmacy and Nutrition, University of Saskatchewan, Saskatoon, SK, Canada
[2]Department of Chemistry, University of Saskatchewan, Saskatoon, SK, Canada

ABSTRACT Gemini surfactant nanoparticles have been successfully used as nonviral gene delivery systems. Using electrospray ionization (ESI) quadrupole time-of-flight (Qq-ToF) hybrid tandem mass spectrometry (MS/MS), the authors elucidated the molecular structure of 10 novel diquaternary ammonium gemini surfactants, including the establishment of their MS/MS fingerprints. The gemini surfactants tested belong to two different structural families: G12-s and G18:1-s, where "s" corresponds to the spacer length. Similarities and differences in the fragmentation patterns within each gemini surfactant family and between them were also identified. In addition, single-stage MS analysis showed that mass accuracy was less than 5 ppm for all compounds.

KEYWORDS fragmentation pattern, gemini surfactants, tandem mass spectrometry, time-of-flight mass spectrometry

INTRODUCTION

Nanoparticles have garnered attention for their possible use in nonviral gene delivery systems to treat both genetically based and infectious diseases.[1–7] This attention is due to their relatively low cost of preparation,[8] ability to target specific tissues,[9–11] capability to encapsulate and carry large amounts of genetic material,[12] and increased safety when compared to viral vectors.[13] One particular group of nanoparticles that has gained attention for its ability to deliver genetic material into cells is the group of gemini surfactants.

Gemini surfactants are constructed by covalently binding the hydrophobic tail regions, (*t*), directly to or near the polar head group of both termini of a spacer molecule, (*s*), to produce a tail–spacer–tail structure, (*t-s-t*). The gemini surfactants tested in this study are given identifier names comprising gemini surfactant ("G"), carbon tail length ("*t*"), and carbon spacer length ("*s*") (G*t-s*) (Fig. 1).[14] The chemical variation in both the spacer and tail regions allows for the production of a wide variety of gemini surfactants. The efficiency of each compound to form a compact and stabilized morphology around naked deoxyribonucleic acid (DNA)[15] depends

Received 13 May 2009; accepted 7 August 2009.

Address correspondence to Anas El-Aneed, College of Pharmacy and Nutrition, University of Saskatchewan, Canada S7H3R3. E-mail: Anas.El-Aneed@usask.ca

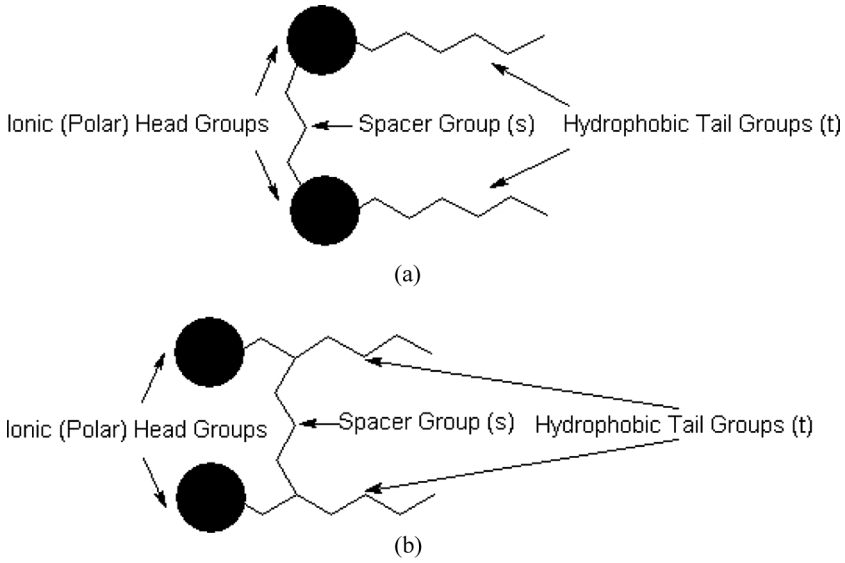

FIGURE 1 **The general structure of a gemini surfactant (a) that contains a spacer group that is covalently bonded directly to the ionic (polar) head group and (b) that contains a spacer group that is covalently bonded to the hydrophobic tail group near the ionic (polar) head groups.**

upon its ability to self-assemble, which in turn depends upon its critical micelle concentration values,[16] how closely its hydrophobic groups can pack together[17,18] and the efficiency with which the positively charged nitrogen interacts with the DNA phosphate groups.[15,19] Stabilization and compaction of DNA-gemini surfactant complexes is driven by entropy and results from the electrostatic interactions between the polyanionic DNA backbone and the dicationic gemini surfactants as well as the hydrophobic interactions between the gemini surfactants' two apolar hydrocarbon tails.[20]

The two G*t-s* gemini surfactant nanoparticle families used in this study comprised *N,N*-bis (dimethyl'alkyl')-α,ω-'alkane'diammonium dibromide ($[C_{12}H_{[(2\bullet12)+1]}]\ N^{+}(CH_3)_2\ (CH_2)_s\ N^{+}(CH_3)_2\ [C_{12}H_{[(2\bullet12)+1]}] \bullet 2Br^{-}$) (Fig. 2a) and *N,N*-bis (dimethyl'alk-σ-ene')-α,ω-'alkane'diammonium

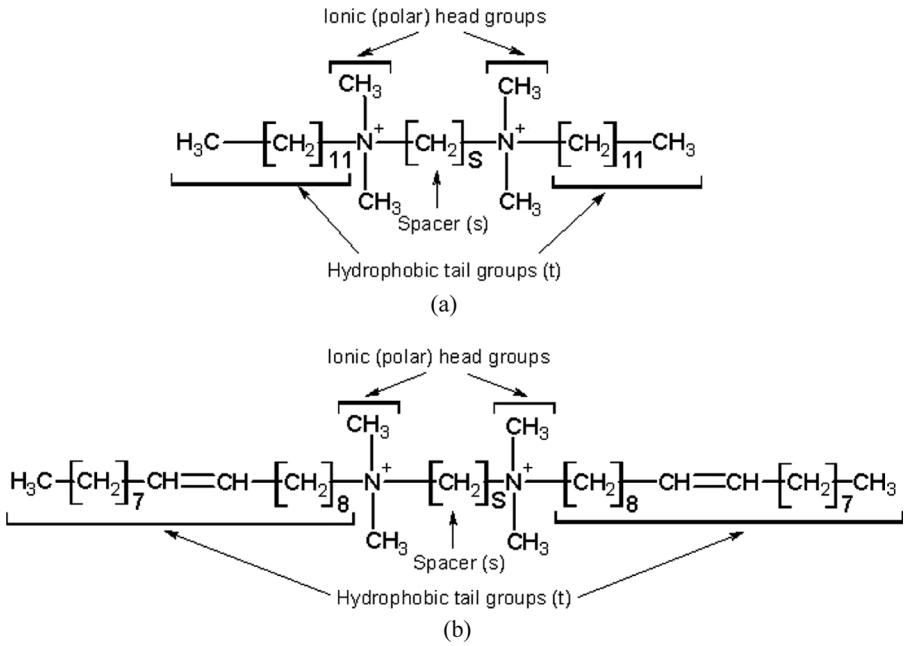

FIGURE 2 **The general structure of the Gemini surfactants (a) G12-s or *N,N*-bis(dimethyldodecyl)-1,'s'-'alkan'diammonium and (b) G18:1-s or *N,N*-bis(dimethylheptadec-9-ene)-1,'s'-'alkan'diammonium ('s' and 'alkan' refer to the carbon composition of the spacer region).**

diammonium dibromide ($[C_{18}H_{[(2\bullet18)-1]}]\ N^{+}(CH_3)_2(CH_2)_s\ N^{+}(CH_3)_2[C_{18}H_{[(2\bullet18)-1]}] \bullet 2Br^{-}$) (Fig. 2b) salts. Gemini surfactants belong to the self-assembling, lipid-based nanoparticle drug delivery systems.[21,22] They have been used as nanomaterials for nearly two decades[22] and are well-characterized.[23,24] For example, analysis of the size distribution of many diquaternary ammonium gemini surfactants was performed by either nonnegative least-squares algorithmic (NNLS) analysis (measurement of the light scattered by particles in solution illuminated by a laser beam ($\gamma = 1731$)), zeta potential, or atomic force microscopy with size distribution being assessed as between 100 and 200 ± 10 nm.[23,24] In addition, these polycationic molecules have been successfully employed for both *in vitro* and *in vivo* gene delivery applications.[13,25–28] For example, topical transfection of the IFNγ gene into mouse epidermis using the G12-3 and G16-3 gemini surfactants produced a 250–450% increase in levels of IFNγ in the epidermis compared to naked IFNγ genes.[9,23,24]

Mass spectrometry (MS) is a powerful analytical tool that has been used for both qualitative and quantitative applications.[29–32] Single-stage MS and tandem mass spectrometry (MS/MS) can be utilized for structural determination and MS/MS fingerprint identification.[33] For example, using electrospray ionization (ESI), the MS/MS analysis of 18 novel cholesteryl neoglycolipids, used in liposomes-based gene delivery, resulted in the formation of specific common fingerprint fragments regardless of the nature of the sugar moiety or the spacer group that linked the carbohydrate portion to the lipid cholesteryl moiety.[34] In addition, the unknown molecular structure of lipid A, isolated from the *A. salmonicida* lipopolysaccharide, was established by single-stage MS and MS/MS analysis using ESI ionization and quadrupole time-of-flight (Qq-ToF) MS/MS techniques.[35,36] Similarly, the fragmentation routes of morphine antagonists were precisely determined using ESI-Qq-ToF MS/MS.[32] MS/MS fingerprints allow for the rapid screening of biological materials and environmental samples to determine the absence or presence of particular compounds within the tested samples. In addition, MS/MS data can be used to develop MS-based quantification methods.

This paper describes the findings regarding the elucidation of the exact molecular structure for the G12-*s* and G18:1-*s* families of gemini surfactants as well as the identification of the fingerprint product ions for all 10 gemini surfactants analyzed and their fragmentation pattern using MS/MS. The analysis of an additional 25 gemini surfactants belonging to three different structural gemini families are currently being investigated.

MATERIALS AND METHODS

The G*t-s* gemini surfactant nanoparticles that we analyzed were obtained from Dr. Ronald E. Verrall's research group in the Department of Chemistry at the University of Saskatchewan. The compounds are from the G12-*s* and G18:1-*s* families (Fig. 2) and include the following:

1. G12-2 or *N,N*-bis(dimethyldodecyl)-1,2-ethanediammonium dibromide
2. G12-4 or *N,N*-bis(dimethyldodecyl)-1,4-butanediammonium dibromide
3. G12-6 or *N,N*-bis(dimethyldodecyl)-1,6-hexanediammonium dibromide
4. G12-8 or *N,N*-bis(dimethyldodecyl)-1,8-octanediammonium dibromide
5. G12-10 or *N,N*-bis(dimethyldodecyl)-1,10-decanediammonium dibromide
6. G12-12 or *N,N*-bis(dimethyldodecyl)-1,12-dodecanediammonium dibromide
7. G12-16 or *N,N*-bis(dimethyldodecyl)-1,16-hexadecanediammonium dibromide
8. G18:1-2 or N,N-bis(dimethyloctadec-9-ene)-1,2-ethanediammonium dibromide
9. G18:1-3 or N,N-bis(dimethyloctadec-9-ene)-1,3-propanediammonium dibromide
10. G18:1-6 or N,N-bis(dimethyloctadec-9-ene)-1,6-hexanediammonium dibromide.

Gemini surfactant solutions were prepared to a concentration of 3 mM in methanol and water (50:50 v:v) containing 0.1% trifluoroacetic acid (99% purity) and stored at −20°C. Each sample was further diluted 4000× and 5000× at the time of analysis using the same mixed solvent.

To minimize associated errors in mass measurements, internal calibration was employed. We opted for using doubly charged calibrants since the tested gemini surfactants are doubly charged species. Therefore, we used both [Glu^1]-Fibrinopeptide B, Human (amino acid sequence EGVNDNEEGFFSAR,

$[M+2H]^{2+}$ m/z 785.8421, $C_{66}H_{95}N_{19}O_{26}$, BaChem Bioscience Inc., King of Prussia, PA, USA) and *N,N*-bis(dimethyldodecyl)-1,2-ethanediammonium dibromide ($[M]^{2+}$ m/z 234.2685). The later compound was chosen because its m/z value fell within the m/z range of the tested compounds. Its molecular structure was previously confirmed by elemental analysis, NMR and purity evaluation.[37,38]

The MS instrument was operated in the positive ion mode with the following parameters: declustering potential of 40.0 V and focusing potential of 120.0 V. The collision gas used during MS/MS experiments was argon and many MS/MS experiments were performed for each compound with the collision energy (CE) values varying between 15–100 eV. CE was optimized in order to generate product ions while ensuring that the molecular ion remained abundant. Sample aliquots, between 100 μL and 500 μL, were infused into the mass spectrometer with an integrated Harvard Syringe Pump at a rate of 10 μL/min using the Turbo Ionspray source; 5.5 kV at a temperature between 80° and 100°C.

A Micromass Quattro II quadrupole-hexapole-quadrupole mass spectrometer (QHQ-MS) was used to confirm the fragmentation pattern. The instrument was operated in the positive ion mode with the following parameters: infusion rate of 10 μL/min, source temperature of 140°C, HV lens voltage of 0.71 kV and capillary voltage of 3.50 V. The cone voltage was set at 70 V to induce in source fragmentation of the compounds. The collision gas used during MS/MS experiments was argon and the collision energy was set between 15 and 50 eV in order to generate product ions while ensuring that the precursor ion remained abundant.

RESULTS AND DISCUSSION

Single-Stage QqToF MS and Tandem QqToF MS/MS Analysis

The results from the single-stage QqToF MS analysis are assessed by comparing the observed mass to charge ratio (m/z) values with the calculated m/z values, producing mass accuracies[39] less than 5 ppm for all gemini surfactants using internal calibration (Table 1). This confirms the projected molecular composition of each gemini surfactant, which includes the presence of two nitrogen atoms in all compounds.[9,12,23,37,38]

TABLE 1 Mass Accuracies of Compounds Using the Calculated and Observed Mass-To-Charge Ratio (m/z) Values

Compound name (Gt-s)	Molecular formula (M)	Calculated (m/z)	Observed (m/z)	Mass accuracy (PPM)
G12-2	$C_{30}H_{66}N_2$	227.2607	227.2604	−1.3
G12-4	$C_{32}H_{70}N_2$	241.2769	241.2764	−2.1
G12-6	$C_{34}H_{74}N_2$	255.2910	255.2920	3.9
G12-8	$C_{36}H_{78}N_2$	269.3084	269.3077	−2.6
G12-10	$C_{38}H_{82}N_2$	283.3230	283.3233	1.1
G12-12	$C_{40}H_{86}N_2$	297.3393	297.3390	−1.0
G12-16	$C_{44}H_{94}N_2$	326.3691	326.3703	3.7
G18:1-2	$C_{42}H_{86}N_2$	309.3393	309.3390	−1.0
G18:1-3	$C_{43}H_{88}N_2$	316.3458	316.3468	3.2
G18:1-6	$C_{46}H_{94}N_2$	337.3704	337.3703	−0.3

The variation in spacer lengths within both the G12-*s* and G18:1-*s* gemini surfactant families produces distinctive product ions within each MS/MS spectra (Figs. 3a and 4a). These product ions, although specific for each gemini surfactant, follow a similar fragmentation pattern for each family which is seen by the incremental increases in the gemini surfactant's MS/MS product ion's m/z values that are equal to the increase in its molecular ion $[M]^{2+}$ m/z values (Tables 2 and 3). The unique spectra and fragmentation patterns produced by both G12-16 (Figs. 3a and 3b), representative of the G12-*s* family, and G18:1-6 (Figs. 4a and 4b), representative of the G18:1-*s* family, are discussed below. These two compounds produced the most complex spectra for their respective families. All other compounds produced similar fragments as shown in Tables 2 and 3.

QqToF MS/MS Analysis of G12-16 Gemini Surfactant

In all G12-*s* gemini surfactant nanoparticles, the unique fragmentation pattern starts with the formation of a singly and/or doubly charged product ion(s) that results from the loss of the twelve carbon tail moiety. In G12-16, this creates the singly charged species $[M\text{-}C_{12}H_{25}]^+$ of m/z 481.55 (**2**) and/or the doubly charged product ion $[M\text{-}C_{12}H_{24}]^{2+}$ of m/z 241.28 (**2′**) (Table 2 and Figs. 3a and 3b). The loss of the hydrocarbon tail in G12-16 occurs by two

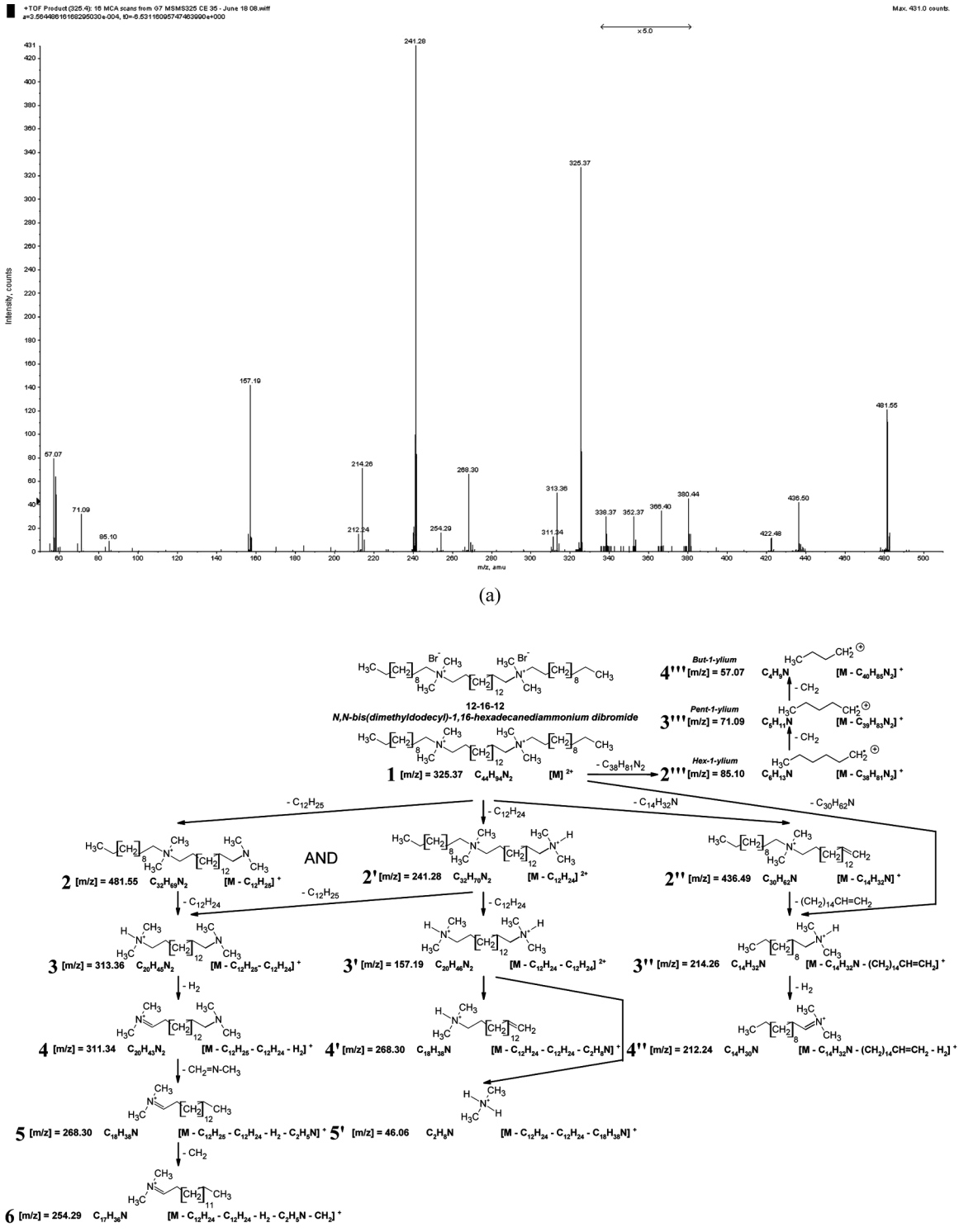

(a)

(b)

FIGURE 3 **G12-16 produced the most fragments of the G12-s family and is therefore representative of it. The (a) MS/MS spectra of G12-16 and (b) the fragmentation pattern show a number of diagnostic fragments that can be utilized for structural identification. A number of nondiagnostic fragments were also produced from 2″ $[M\text{-}C_{14}H_{32}N]^+$ but were not included in Figure 3b.**

mechanisms and is dependent upon the product ion(s) formed; singly or doubly charged. The elimination of a neutral CH_2=CH $(CH_2)_9$-CH_3 (dodec-1-ene), due to a proton transfer to the nitrogen atom, produces the doubly charged ion observed at m/z 241.28 while the heterolytic cleavage of the N-C bond forms the singly charged ion, m/z 481.55. The second elimination product

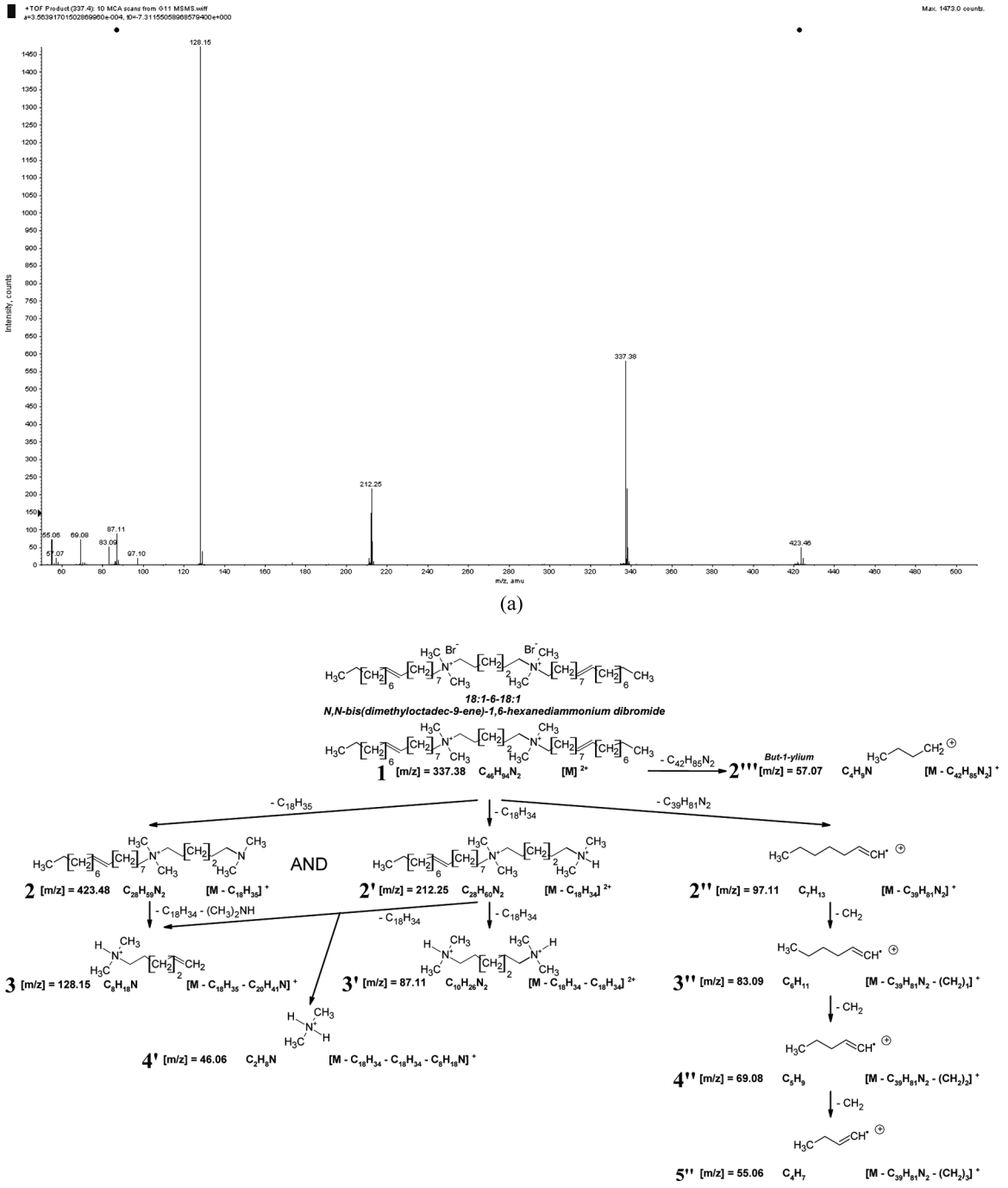

FIGURE 4 **G18:1-6 produced the most fragments of the G18:1-s family and is therefore representative of it. The (a) MS/MS spectra of G18:1-6 and (b) the fragmentation pattern show a number of diagnostic fragments that can be utilized for structural identification.**

(m/z 481.55) should, in theory, produce a complementary ion of the tail the region with a theoretical m/z 169.19. However, this ion was not observed during MS/MS of the precursor ions using either QqToF or QHQ analysis under various experimental conditions, regardless of the collision energy. It is possible that the ion expected at m/z 169.19 was instantly formed and neutralized via proton transfer from other species within the collision cell. As discussed below and shown in Table 2, only short aliphatic radical ions were observed at m/z 85.10 (**2**‴), 71.09 (**3**‴) and 57.07 (**4**‴) (Figs. 3a and 3b), which supports the notion that longer singly charged alkyl chains were neutralized.

Following the same mechanism described in the previous section, the loss of the second twelve

TABLE 2 **Fragment Identification and Corresponding m/z Value for Each Gemini Surfactant Compound in the G12-s Family**

Compound	G12-2	G12-4	G12-6	G12-8	G12-10	G12-12	G12-16	
Molecular formula (M)	($C_{30}H_{66}N_2$)	($C_{32}H_{70}N_2$)	($C_{34}H_{74}N_2$)	($C_{36}H_{78}N_2$)	($C_{38}H_{82}N_2$)	($C_{40}H_{86}N_2$)	($C_{44}H_{94}N_2$)	
Spacer region (s)	(C_2H_4)	(C_4H_8)	(C_6H_{12})	(C_8H_{16})	($C_{10}H_{20}$)	($C_{12}H_{24}$)	($C_{16}H_{32}$)	
Collision energy (eV)	16	25	25	30	30	30	35	
Product ions	(m/z)	(m/z)	(m/z)	(m/z)	(m/z)	(m/z)	(m/z)	#
$[M]^{2+}$	227.26	241.28	255.30	269.31	283.32	297.35	325.37	**1**
$[M\text{-}C_{12}H_{25}\ ]^{+}$	285.32	313.39	341.41	369.42	397.45	425.49	481.55	**2**
$[M\text{-}C_{12}H_{25}\text{-}C_{12}H_{24}]^{+}$				201.12	229.26	257.30	313.36	**3**
$[M\text{-}C_{12}H_{25}\text{-}C_{12}H_{24}\text{-}H_2]^{+}$				199.22	227.25	255.29	311.34	**4**
$[M\text{-}C_{12}H_{25}\text{-}C_{12}H_{24}\text{-}H_2\text{-}C_2H_5N]^{+}$	72.08	100.11	128.15	156.17	184.20	212.32	268.30	**5**
$[M\text{-}C_{12}H_{25}\text{-}C_{12}H_{24}\text{-}H_2\text{-}C_2H_5N\text{-}CH_2]^{+}$							254.29	**6**
$[M\text{-}C_{12}H_{24}\ ]^{2+}$	143.17	157.19	171.20	185.22	199.23	213.25	241.28	**2′**
$[M\text{-}C_{12}H_{24}\text{-}C_{12}H_{24}]^{+}$			87.11	101.12	115.14	129.16	157.19	**3′**
$[M\text{-}C_{12}H_{24}\text{-}C_{12}H_{24}\text{-}C_2H_8N]^{+}$	72.08	100.11	128.15	156.17	184.20	212.32	268.30	**4′**
$[M\text{-}C_{12}H_{24}\text{-}C_{12}H_{24}\text{-}('s'+C_2H_6N)]^{+}$	46.06	46.06	46.06	46.06	46.06	46.06	46.06	**5′**
$[M\text{-}C_{14}H_{32}N\ ]^{+}$						380.44	436.49	**2″**
$[M\text{-}C_{14}H_{32}N\text{-}(CH_2)_{s\text{-}2}CH{=}CH_2]^{+}$	214.09	214.09	214.10	214.24	214.26	214.25	214.26	**3″**
$[M\text{-}C_{14}H_{32}N\text{-}(CH_2)_{s\text{-}2}CH{=}CH_2\text{-}H_2]^{+}$			212.24	212.24	212.24	212.24	212.24	**4″**
$[M\text{-}C_{22}H_{48}N_2\text{-}'s']^{+}$	85.10	85.10	85.10	85.10	85.10	85.10	85.10	**2‴**
$[M\text{-}C_{23}H_{50}N_2\text{-}'s']^{+}$	71.09	71.09	71.09	71.09	71.09	71.09	71.09	**3‴**
$[M\text{-}C_{24}H_{52}N_2\text{-}'s']^{+}$	57.07	57.07	57.07	57.07	57.07	57.07	57.07	**4‴**

TABLE 3 **Fragment Identification and Corresponding *m/z* Value for Each Gemini Surfactant Compound in the G18:1-s Family**

Compound	G18:1–2	G18:1–3	G18:1–6	
Molecular formula (M)	($C_{42}H_{86}N_2$)	($C_{43}H_{88}N_2$)	($C_{46}H_{94}N_2$)	
Spacer region (s)	(C_2H_4)	(C_3H_6)	(C_6H_{12})	
Collision energy (eV)	20	25	31	
Product ions	(*m/z*)	(*m/z*)	(*m/z*)	#
$[M]^{2+}$	309.34	316.35	337.38	**1**
$[M\text{-}C_{18}H_{35}]^{+}$	367.41	381.43	423.48	**2**
$[M\text{-}C_{18}H_{35}\text{-}C_{18}H_{34}\text{-}(CH_3)_2NH]^{+}$	72.08	86.10	128.15	**3**
$[M\text{-}C_{18}H_{34}\ ]^{2+}$		191.35	212.25	**2′**
$[M\text{-}C_{18}H_{34}\text{-}C_{18}H_{34}]^{2+}$			87.11	**3′**
$[M\text{-}C_{18}H_{34}\text{-}C_{18}H_{34}\text{-}('s'+(CH_3)_2N]^{+}$	46.06	46.06	46.06	**4′**
$[M\text{-}C_{30}H_{63}N_2\text{-}S]^{+}$	97.10	97.10	97.11	**2″**
$[M\text{-}C_{31}H_{65}N_2\text{-}S]^{+}$	83.09	83.09	83.09	**3″**
$[M\text{-}C_{32}H_{67}N_2\text{-}S]^{+}$	69.08	69.08	69.08	**4″**
$[M\text{-}C_{33}H_{69}N_2\text{-}S]^{+}$	55.06	55.06	55.06	**5″**
$[M\text{-}C_{33}H_{67}N_2\text{-}S]^{+}$	57.07	57.07	57.07	**2‴**

carbon tail produces a doubly charged product ion $[M\text{-}C_{12}H_{24}\text{-}C_{12}H_{24}]^{2+}$, at *m/z* 157.19 (**3′**), and the singly charged ion $[M\text{-}C_{12}H_{25}\text{-}C_{12}H_{24}]^{2+}$, at *m/z* 313.36 (**3**), (Table 2 and Figs. 3a and 3b). The origin of the fragment ions was confirmed via MS/MS analysis using QHQ instrument. QHQ, contrary to QqToF, is able to generate strong "in source" fragmentation and hence this allowed us to authenticate the proposed fragmentation pathways and the order in which ions are formed (Table 4). An additional aminium ion that is produced by the loss of H_2 from the singly charged ion, $[M\text{-}C_{12}H_{25}\text{-}C_{12}H_{24}]^{2+}$ (**3**), results in the formation of a double bond between the terminal carbon of the spacer and the nitrogen; $[M\text{-}C_{12}H_{24}\text{-}C_{12}H_{25}\text{-}H_2]^{2+}$ at *m/z* 311.34 (**4**) (Table 2 and Figs. 3a and 3b). The loss of a neutral CH_2=N-CH_3 (*N*-methylidenemethanamine) from the singly charged, *m/z* 311.34 (**4**) produces the product ion of $[M\text{-}C_{12}H_{25}\text{-}C_{12}H_{24}\text{-}H_2\text{-}C_2H_5N]^{+}$ at *m/z* 268.3 (**5**) and subsequent elimination of a CH_2 yields the ion, $[M\text{-}C_{12}H_{25}\text{-}C_{12}H_{24}\text{-}H_2\text{-}C_2H_5N\text{-}CH_2]^{+}$, at *m/z* 254.29 (**6**) (Tables 2 and 4 and Figs. 3a and 3b). The diagnostic product ions represented by $[M\text{-}C_{12}H_{25}\text{-}C_{12}H_{24}\text{-}H_2\text{-}C_2H_5N]^{+}$(**5**) (Fig. 3b) are observed in all G12-*s* gemini surfactants nanoparticles presented in Table 2.

TABLE 4 **Tandem Mass Spectrometric Analysis Using an HQH instrument. The Formation of Diagnostic Ions During MS/MS Analysis Confirmed the Fragmentation Pathway for Each Gemini Surfactant Structural Family**

MS/MS ions of G12-16	Diagnostic MS/MS ions produced
241.28	313, 311, 268, 254, 214, 212, 157, 46
481.55	313, 311, 268, 254, 214, 212
157.19	268, 46
313.36	311, 268, 254
311.00	268
268.30	254
436.49	214, 212
MS/MS Ions of G18:1-6	**Diagnostic MS/MS ions produced**
212.25	128, 87, 46
423.48	128

On the other hand, the doubly charged product ion observed at *m/z* 157.19 (**3′**) is also cleaved at the terminal N-C bond releasing two complementary ions observed at *m/z* 268.3, $[M\text{-}C_{12}H_{24}\text{-}C_{12}H_{24}\text{-}C_2H_8N]^{+}$, (**4′**) and *m/z* 46.06, *N*-methylmethanaminium, (**5′**). Based upon the diagnostic fragments produced by the ions at *m/z* 311.34 (**4**) and 157.19 (**3′**) (Table 4), it can be concluded that two structural isomers exist for the ion observed at m/z 268.3 (5 and 4′) (Figs. 3a and 3b). In a similar mechanism that produces the complementary ions observed at *m/z* 268.3 (4′) and 46.06 (5′), another pair of complementary diagnostic product ions were

produced from the cleavage of the N-C bond within the molecular ion and observed at m/z 436.49 (**2″**) and 214.26 (**3″**) (Table 2 and Fig. 3a & 3b).

Additional nondiagnostic product ions were observed at m/z 422.47, m/z 380.43, m/z 366.41, m/z 352.37, and m/z 338.34 in G12-16 (Fig. 3a). These minor nondiagnostic ions results from the loss of $(CH_2)_n$ and originated from different sources (m/z 481.55, 241.28, 436.49) as confirmed by QHQ analysis (data not shown). Furthermore, nondiagnostic ions are expected and result from the tail region of the G12-s gemini surfactants as a result of their identical nature. Identical fragments seen in the analyzed G12-*s* gemini surfactants are singly charged small product ions, namely, *N,N*-dimethyldodecan-1-aminium (**3″**), *N,N*-dimethyldodec-1-en-1-aminium (**4″**), hex-1-ylium (**2‴**) pent-1-ylium (**3‴**) and but-1-ylium (**4‴**) (Table 2 and Figs. 3a and 3b). It should be noted that the final three small fragment ions can be generated from all ions which contain the gemini surfactant tail region; for illustrative purposes, we opted to present these ions being generated from the molecular ion (Fig. 3b).

QqToF MS/MS Analysis of G18:1-6 Gemini Surfactant

The fragmentation pattern of the G18:1-*s* family of gemini surfactant nanoparticles follows a similar fragmentation pattern to the G12-*s* family and produces singly and/or doubly charged product ion(s) due to the loss of a tail moiety. In G18:1-6, these product ions are observed as $[M\text{-}C_{18}H_{35}]^{2+}$ at m/z 423.48 (**2**) and $[M\text{-}C_{18}H_{34}]^{2+}$ at m/z 212.25 (**2′**) (Table 3 and Figs. 4a and 4b). The subsequent loss of the second tail moiety from m/z 212.25, $[M\text{-}C_{18}H_{34}]^{2+}$, results in the formation of a doubly charged ion $[M\text{-}C_{18}H_{34}\text{-}C_{18}H_{34}]^{+}$ at m/z 87.11 (**3′**) (Table 3 and Figs. 4a and 4b). This doubly charged ion is only observed in G18:1-6. In fact, the doubly charged ion observed at m/z 87.11 (**3′**) is a very minor product ion (Fig. 4a) and therefore it is very likely that its formation is transient and it is relatively unstable due to the close proximity of the positive charges in both G18:1–2 and G18:1–3.

On the other hand, the loss of both tail regions, one bound to a single dimethyl-amino, is observed in all G18:1-*s* gemini surfactant. In G18:1-6, this is observed as, $[M\text{-}C_{18}H_{35}\text{-}C_{20}H_{41}N]^{+}$ at m/z 128.15 (**3**) and it can be formed from $[M\text{-}C_{18}H_{35}]^{+}$ (**2**) due to the dual cleavage of a neutral $CH_3(CH_2)_7CH{=}CH(CH_2)_6CH{=}CH_2$ and $NH(CH_3)_2$. It can also be formed from the ion $[M\text{-}C_{18}H_{34}]^{+}$ (**2′**) via the loss of a neutral $CH_3(CH_2)_7CH{=}CH(CH_2)_6CH{=}CH_2$ and the corresponding singly charged ion m/z 46.06, *N*-methylmethanaminium (4′) (Table 3 and Figs. 4a and 4b). The proposed fragmentation pathways were confirmed via QHQ-MS/MS experiments (Table 4).

Since all G18:1-*s* gemini surfactants contain identical tail regions it is expect that there will be shared fragments within this gemini surfactant family. The presence of a double bond in the tail regions of the G18:1-*s* gemini surfactants results in a double bond also being present in their product ions, producing alk-1-en-1-ylium fragments: hept-1-en-1-ylium (**2″**), m/z 97.11, hex-1-en-1-ylium (**3″**), m/z 83.09, pent-1-en-1-ylium (**4″**), m/z 69.08, and but-1-en-1-ylium (**5″**), m/z 55.06 (Table 3 and Fig. 4a & 4b). Similar to the G12-*s* family, an additional identical fragment seen in all analyzed G18:1-s gemini surfactants: a singly charged but-1-ylium at m/z 57.07 (**2‴**) (Table 3 and Figs. 4a and 4b).

Increased fragmentation complexity is observed, in Tables 2 and 3, as the spacer region length is increased from two to sixteen or two to six carbons in length; with G12-16 and G18:1-6 generating the most complex fragmentation patterns of their respective families (Fig. 3a, 3B, 4a & 4b). However, these spectra possess the fragments that are present in the spectra of other gemini surfactants and therefore they are representative of the G12-*s* and G18:1-*s* gemini surfactant families of nanoparticles, respectively. Within these distinct spectra there is, however, one identical product ion shared by all ten compounds, but-1-ylium at m/z 57.07 (Tables 2 and 3), and several ions among the ten compounds which are structurally conserved; for example, the loss of a single tail fragment, **2** and **2′** (Tables 2 and 3 and Figs. 3a, 3B, 4a and 4b).

CONCLUSIONS

The molecular composition of each G12-*s* and G18:1-*s* gemini surfactant was determined by QqToF-MS analysis. The assessment of the fragmentation pattern for each gemini surfactant was done by QqToF-MS/MS and demonstrated that the gemini surfactants share fragmentation patterns that are

specific to their respective gemini surfactant families. Currently, a study of other gemini surfactant families is taking place with the intent of identifying for each gemini surfactant two to three product ions that have unique m/z values and that will be utilized in multiple-reaction monitoring. Multiple-reaction monitoring utilizes both the precursor ion and the select diagnostic product ions produced for the quantification of the compound. In addition, both the precursor–to–product-ion transition and the retention times of each compound will allow for their exact identification. By identification of both the similarities and differences between each gemini surfactant's product ions, the differing product ions become candidates for use during LC-MS/MS quantification of them and their metabolites in biological samples. By quantification of both the gemini surfactants and their metabolites, an evaluation of their toxicity, bioavailability, and half-life during the course of transfection can be undertaken. Currently, the LC method necessary to separate the gemini surfactants is being designed to quantify individual gemini surfactants in tissue culture extracts.

REFERENCES

1. Bozkir, A.; Saka, O. M. Chitosan-DNA nanoparticles: Effect on DNA integrity, bacterial transformation and transfection efficiency. *Journal of Drug Targeting* **2004**, *12*(5), 281–288.
2. Choi, S. H.; Jin, S. E.; Lee, M. K.; Lim, S. J.; Park, J. S.; Kim, B. G.; Ahn, W. S.; Kim, C. K. Novel cationic solid lipid nanoparticles enhanced p53 gene transfer to lung cancer cells. *European Journal of Pharmaceutics and Biopharmaceutics* **2008**, *68*(3), 545–554.
3. de la Fuente, M.; Seijo, B.; Alonso, M. J. Novel hyaluronic acid-chitosan nanoparticles for ocular gene therapy. *Investigative Ophthalmology and Visual Science* **2008**, *49*(5), 2016–2024.
4. Kaul, G.; Amiji, M. Tumor-targeted gene delivery using poly(ethylene glycol)-modified gelatin nanoparticles: In vitro and in vivo studies. *Pharmaceutical Research* **2005**, *22*(6), 951–961.
5. Martien, R.; Loretz, B.; Schnurch, A. B. Oral gene delivery: Design of polymeric carrier systems shielding toward intestinal enzymatic attack. *Biopolymers* **2006**, *83*(4), 327–336.
6. Moreira, J. N.; Santos, A.; Moura, V.; Pedroso de Lima, M. C.; Simoes, S. Non-viral lipid-based nanoparticles for targeted cancer systemic gene silencing. *Journal of Nanoscience and Nanotechnology* **2008**, *8*(5), 2187–2204.
7. Prabha, S.; Labhasetwar, V. Nanoparticle-mediated wild-type p53 gene delivery results in sustained antiproliferative activity in breast cancer cells. *Molecular Pharmaceutics* **2004**, *1*(3), 211–219.
8. Patil, S. D.; Rhodes, D. G.; Burgess, D. J. DNA-based therapeutics and DNA delivery systems: A comprehensive review. *AAPS Journal* **2005**, *7*(1), E61–E77.
9. Badea, I.; Verrall, R.; Baca-Estrada, M.; Tikoo, S.; Rosenberg, A.; Kumar, P.; Foldvari, M. *In vivo* cutaneous interferon-γ gene delivery using novel dicationic (gemini) surfactant-plasmid complexes. *Journal of Gene Medicine* **2005**, *7*(5), 1200–1214.
10. Dubey, P. K.; Mishra, V.; Jain, S.; Mahor, S.; Vyas, S. P. Liposomes modified with cyclic RGD peptide for tumor targeting. *Journal of Drug Targeting* **2004**, *12*(5), 257–264.
11. Zhang, N.; Chittasupho, C.; Duangrat, C.; Siahaan, T. J.; Berkland, C. PLGA nanoparticle-peptide conjugate effectively targets intercellular cell-adhesion Molecule-1. *Bioconjugate Chemistry* **2008**, *19*(1), 145–152.
12. Wettig, S. D.; Verrall, R. E.; Foldvari, M. Gemini surfactants: A new family of building blocks for non-viral gene delivery systems. *Current Gene Therapy* **2008**, *8*(1), 9–23.
13. Thomas, M.; Klibanov, A. M. Non-viral gene therapy: Polycation-mediated DNA delivery. *Applied Microbiology Biotechnology* **2003**, *62*(1), 27–34.
14. Menger, F. M.; Littau, C. A. Gemini-surfactants: Synthesis and properties. *Journal of the American Chemical Society* **1991**, *113*(4), 1451–1452.
15. Karlsson, L.; van Eijk, M. C. P.; Soderman, O. Compaction of DNA by gemini surfactants: Effects of surfactant architecture. *Journal of Colloid and Interface Science* **2002**, *252*(2) 290–296.
16. Li, J.; Dahanayake, M.; Reierson, R. L.; Tracy, D. J. Topical Compositions and Methods for Treatment of Skin Damage and Aging Using Catecholamines and Related Compounds. U.S. Patent 5,643,586 (1997).
17. Zhu, Y. P.; Masuyama, A.; Kirito, Y. I.; Okahara, M.; Rosen, M. J. Preparation and properties of glycerol-based double or triple-chain surfactants with two hydrophilic ionic groups. *Journal of the American Oil Chemists' Society* **1992**, *69*(7), 626–632.
18. Pinazo, A.; Diz, M.; Solans, C.; Pés, M. A.; Erra, P.; Infante, M. R. Synthesis and properties of cationic surfactants containing a disulfide bond. *Journal of the American Oil Chemists' Society* **1993**, *70*(1), 37–42.
19. Liu, L.; Rosen, M. J. The interaction of some novel diquaternary gemini surfactants with anionic surfactants. *Journal of Colloid and Interface Science* **1996**, *179*(2), 454–459.
20. Matulis, D.; Rouzina, I.; Bloomfield, V. A. Thermodynamics of cationic lipid binding to DNA and DNA condensation: Roles of electrostatics and hydrophobicity. *Journal of the American Chemical Society* **2002**, *124*(25), 7331–7342.
21. Kirby, A. J.; Camilleri, P.; Engberts, J. B. F. N.; Feiters, M. C.; Nolte, R. J. M.; Soderman, O.; Bergsma, M.; Bell, P. C.; Fielden, M. L.; Garcia Rodriguez, C. L.; Guedat, P.; Kremer, A.; McGregor, C.; Perrin, C.; Ronsin, G.; van Eijk, M. C. P. Gemini surfactants: New synthetic vectors for gene transfection. *Angewandte Chemie, International Edition* **2003**, *42*, 1448–1457.
22. Menger, F. M.; Littau, C. A. Gemini surfactants: A new class of self-assembling molecules. *Journal of the American Chemical Society* **1993**, *115*, 10083–10090.
23. Wang, C.; Xingfu, L.; Wettig, S. D.; Badea, I.; Foldvari, M.; Verrall, R. E. Investigation of complexes formed by interaction of cationic gemini surfactants with deoxyribonucleic acid. *Physical Chemistry Chemical Physics* **2007**, *9*, 1616–1628.
24. Badea, I.; Wettig, S.; Verrall, R.; Foldvari, M. Topical non-invasive gene delivery using gemini nanoparticles in interferon-γ-deficient mice. *European Journal of Pharmaceutics and Biopharmaceutics* **2007**, *65*(3), 414–422.
25. Dauty, E.; Remy, J. S.; Blessing, T.; Behr, J. P. Dimerizable cationic detergents with a low CMC condense plasmid DNA into nanometric particles and transfect cells in culture. *Journal of the American Chemical Society* **2001**, *123*(38), 9227–9234.
26. Wettig, S. D.; Badea, I.; Donkuru, M.; Verrall, R. E.; Foldvari, M. Structural and transfection properties of amine-substituted gemini surfactant-based nanoparticles. *Journal of Gene Medicine* **2007**, *9*(8), 649–658.
27. Fielden, M. L.; Perrin, C.; Kelmer, A.; Bergsma, M.; Stuart, M. C.; Camilleri, P.; Engberts, J. B. F. N. Sugar-based tertiary amino gemini surfactants with a vesicle-to-micelle transition in the endosomal pH range mediate efficient transfection in vitro. *European Journal of Biochemistry* **2001**, *268*(5), 1269–1279.

28. Wettig, S. D.; Badea, I.; Donkuru, M. Substitution effects in gemini surfactants: Application to DNA transfection. Unpublished manuscript in preparation in 2008.
29. Calvo, P.; Gouritin, B.; Villarroyo, H.; Eclancher, F.; Giannavola, C.; Klein, C.; Andreux, J. P.; Couvreur, P. Quantification and localization Pegylated polycyanoacrylate nanoparticles in brain and spinal cord during experimental allergic encephalomyelitis in the rat. *European Journal of Neuroscience* **2002**, *15*(8), 1317–1326.
30. Kim, M. S.; Jin, S. J.; Kim, J. S.; Park, H. J.; Song, H. S.; Neubert, R. H. H.; Hwang, S. J. Preparation, characterization and in vivo evaluation of amorphous atorvastatin calcium nanoparticles using supercritical antisolvent process. *European Journal of Pharmaceutics and Biopharmaceutics* **2008**, *69*(2), 454–465.
31. Wood, M.; De Boeck, G.; Samyn, N.; Morris, M.; Cooper, D. P.; Maes, R. A. A.; De Bruijn, E. A. Development of a rapid and sensitive method for the quantification of amphetamines in human plasma and oral fluid by LC-MS/MS. *Journal of Analytical Toxicology* **2003**, *27*(1), 78–87.
32. Joly, N.; El Aneed, A.; Martin, P.; Cecchelli, R.; Banoub, J. Structural determination of the novel fragmentation routes of morphine opiate receptor antagonists using electrospray ionization quadrupole time-of-flight tandem mass spectrometry. *Rapid Communications in Mass Spectrometry* **2005**, *19*(21), 3119–3130.
33. Nagele, E.; Moritz, R. Structure elucidation of degradation products of the antibiotic amoxicillin with ion trap MSn and accurate mass determination by ESI TOF. *Journal of the American Society for Mass Spectrometry* **2005**, *16*(10), 1670–1676.
34. El-Aneed, A.; Banoub, J.; Koen-Alonso, M.; Boullanger, P.; Lafont, D. Establishment of mass spectrometric fingerprints of novel synthetic cholesteryl neoglycolipids: The presence of a unique C-glycoside species during electrospray ionization and during collision-induced dissociation tandem mass spectrometry. *Journal of the American Society for Mass Spectrometry* **2007**, *18*(2), 294–310.
35. Wang, Z.; Li, J.; Altman, E. Structural characterization of the lipid A region of *Aeromonas salmonicida* subspecies salmonicida lipopolysaccharide. *Carbohydrate Research* **2006**, *341*(17), 2816–2825.
36. El-Aneed, A.; Banoub, J. Elucidation of the molecular structure of lipid A isolated from both a rough mutant and a wild strain of *Aeromonas salmonicida* lipopolysaccharides using electrospray ionization quadrupole time-of-flight tandem mass spectrometry. *Rapid Communications in Mass Spectrometry* **2005**, *19*(12), 1683–1695.
37. Wettig, S. D. Studies of the Interaction of Gemini Surfactants with Polymers and Triblock Copolymers. Ph.D. Thesis, University of Saskatchewan, Saskatoon, Canada, 2000.
38. Jenkins, K. M. Thermodynamic Studies of Bis(quaternaryammonium) and (N-alkyl-) Ionic Surfactants. M.S. Thesis, University of Saskatchewan, Saskatoon, Canada, 2000.
39. Domon, B.; Aebersold, R. Mass spectrometry and protein analysis. *Science* **2006**, *312*(5771), 212–217.